Article

Complex Mechanism of the Gas Phase Reaction between Formic Acid and Hydroxyl Radical. Proton Coupled Electron Transfer versus Radical Hydrogen Abstraction Mechanisms

Josep M. Anglada

J. Am. Chem. Soc., **2004**, 126 (31), 9809-9820• DOI: 10.1021/ja0481169 • Publication Date (Web): 20 July 2004

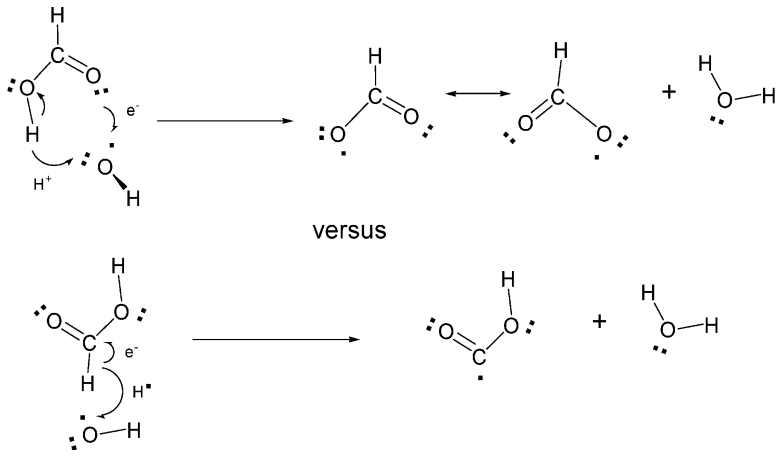

More About This Article

Additional resources and features associated with this article are available within the HTML version:

- Supporting Information
- Links to the 3 articles that cite this article, as of the time of this article download
- Access to high resolution figures
- Links to articles and content related to this article
- Copyright permission to reproduce figures and/or text from this article

View the Full Text HTML

J|A|C|S
ARTICLES
Published on Web 07/20/2004

Complex Mechanism of the Gas Phase Reaction between Formic Acid and Hydroxyl Radical. Proton Coupled Electron Transfer versus Radical Hydrogen Abstraction Mechanisms

Josep M. Anglada

Contribution from the Departament de Química Orgànica Biològica, Institut d'Investigacions Químiques i Ambientals de Barcelona., IIQAB - CSIC. c/ Jordi Girona 18, E08034 Barcelona, Spain

Received April 1, 2004; E-mail: anglada@iiqab.csic.es

Abstract: The gas phase reaction between formic acid and hydroxyl radical has been investigated with high level quantum mechanical calculations using DFT-B3LYP, MP2, CASSCF, QCISD, and CCSD(T) theoretical approaches in connection with the 6-311+G(2df,2p) and aug-cc-pVTZ basis sets. The reaction has a very complex mechanism involving several elementary processes, which begin with the formation of a reactant complex before the hydrogen abstraction by hydroxyl radical. The results obtained in this investigation explain the unexpected experimental fact that hydroxyl radical extracts predominantly the acidic hydrogen of formic acid. This is due to a mechanism involving a proton coupled electron-transfer process. The calculations show also that the abstraction of formyl hydrogen has an increased contribution at higher temperatures, which is due to a conventional hydrogen abstraction radical type mechanism. The overall rate constant computed at 298 K is 6.24×10^{-13} cm^3 molecules^{-1} s^{-1}, and compares quite well with the range from 3.2 ± 1 to $4.9 \pm 1.2 \times 10^{-13}$ cm^3 molecules^{-1} s^{-1}, reported experimentally.

Introduction

A detailed knowledge of the gas-phase reaction of formic acid with hydroxyl radical is of great interest because their importance in atmospheric chemistry. HCOOH is the most abundant carboxylic acid in the troposphere,[1−6] and their main chemical sink is the reaction with OH radical. The presence of formic acid in the troposphere comes from different sources, that include direct emissions from biogenic compounds, photochemical oxidation of volatile organic compounds, biomass burning, automobile exhaust, or as a product in the ozonolysis of several alkenes such ethane, propene and isoprene.[7−16]

Beyond its intrinsic importance, the knowledge of this reaction has also interest because it may serve as a prototype reaction for a complete understanding for the reactivity of atmospheric acids with hydroxyl radicals.

In general, hydroxyl radical reacts with nonradical atmospheric species by extracting hydrogen atoms from the molecular reagent. In the case of formic acid, there are two H atoms that can be extracted and the following two reactions can be envisaged.

$$HCOOH + OH \rightarrow HCOO + H_2O \quad (1)$$

$$HCOOH + OH \rightarrow HOCO + H_2O \quad (2)$$

Experimental studies by Zetzsch et al.,[17] Wine et al.,[18] Jolly et al.,[19] Dagaut et al.[20] and Singleton et al.[21] have been reported in the literature in order to provide the rate constant and to elucidate the reaction mechanism. The measured kinetic rate constant obtained by the different authors are in a very good agreement (among 3.2 ± 1 and $4.9 \pm 1.2 \times 10^{-13}$ cm^3 molecules^{-1} s^{-1} at 298 K), and it was found to be nearly independent of the temperature. Moreover, a strong isotopic effect was also found when the acidic H is substituted by D, whereas the isotopic substitution of the formyl hydrogen does have any effect on the rate constant. In addition, the reactivity

(1) Legrand, M.; Angelis, M. D. *J. Geophys. Res.* **1995**, *100*, 1445.
(2) Grosjean, D. *Environ. Sci. Technol.* **1989**, *23*, 1506.
(3) Puxbaum, H.; Rosenberg, C.; Gregori, M.; Lanzerstorfer, C.; Ober, E.; Winiwarter, W. *Atmos. Environ.* **1988**, *22*, 1841.
(4) Sanhueza, E.; Santana, M.; Hermoso, M. *Atmos. Environ.* **1992**, *26A*, 1421.
(5) Granby, K.; Christensen, C. S.; Lohse, C. *Atmos. Environ.* **1997**, *31*, 1403.
(6) Kesselmeier, J. *J. Atmos. Chem.* **2001**, *39*, 219.
(7) Talbot, R. W.; Beecher, K. M.; Harriss, R. C.; III, W. C. *J. Geophys. Res.* **1988**, *93*, 1638.
(8) Talbot, R. W.; Andreae, M. O.; Berresheim, H.; Jacob, D.; Beecher, H. M. *J. Geophys. Res.* **1990**, *95*, 16799.
(9) Kawamura, K.; Ling, L.; Kaplan, I. R. *Environ. Sci. Technol.* **1985**, *19*, 1082.
(10) Su, F.; Calvert, G.; Shaw, H. H. *J. Phys. Chem.* **1980**, *84*, 239.
(11) Jacob, D. J.; Wofsy, S. C. *J. Geophys. Res.* **1988**, *93*, 1477.
(12) Neeb, P.; Horie, O.; Moortgat, G. K. *J. Phys. Chem. A* **1998**, *102*, 6778.
(13) Grosjean, E.; Andrade, J. B. d.; Grosjean, D. *Environ. Sci. Technol.* **1996**, *30*, 975.
(14) Atkinson, R.; Finlayson, B. J.; Jr., J. N. P. *J. Am. Chem. Soc.* **1973**, *95*, 7592.
(15) Atkinson, R. *Atmos. Environ.* **1990**, *24A*, 1.
(16) Granby, K.; Egelov, A. H.; Nielsen, T.; Lohse, C. *J. Atmos. Chem.* **1997**, *28*, 195.
(17) Zetzsch, C.; Stuhl, F. In *Proceeding of the Second European Symposium*; Versino, B., Ott, H., Eds.; Reidel: Dordrecht, 1982; p 129.
(18) Wine, P. H.; Astalos, R. J.; III, R. L. M. *J. Phys. Chem.* **1985**, *89*, 2620.
(19) Jolly, G. S.; McKenney, D. J.; Singleton, D. L.; Paraskevopoulos, G.; Bossard, A. R. *J. Phys. Chem.* **1986**, *90*, 6557.
(20) Dagaut, P.; Wallington, T. J.; Liu, R.; Kurylo, M. J. *Int. J. Chem. Kinet.* **1988**, *20*, 331.
(21) Singleton, D. L.; Paraskevopoulos, G.; Irwin, R. S.; Jolly, G. S.; Mckenney, D. J. *J. Am. Chem. Soc.* **1988**, *110*, 7786.

10.1021/ja0481169 CCC: $27.50

of OH with formic acid dimmer is lower than that of the monomer. These results lead to the conclusion that hydroxyl radical abstracts predominantly the acidic hydrogen, but this finding was unexpected because in HCOOH the strength of the C−H bond is smaller than that of the O−H bond (the experimental bond dissociation energies (BDE) of these bonds are 96.2 ± 0.7 and 112.2 ± 3.1 kcal/mol, respectively).[22] In view of these facts, Singleton et al.[21] suggested that the reaction occurs predominantly by formation of a pre-reactive hydrogen bonded adduct between OH and formic acid, followed by the H transfer to the hydroxyl group (reactions 3). They also suggested that a direct hydrogen abstraction from the formyl group could make a contribution to the overall rate constant.

$$HCOOH + OH \rightleftharpoons Adduct \rightarrow HCOO + H_2O \qquad (3)$$

In fact, it has been demonstrated very recently that the pre-reactive hydrogen bond intermediates play an important role in atmospheric bimolecular reactions, so that these reactant complexes may have a key influence on the rate constant and on its dependence on temperature and pressure.[23−25]

Despite the atmospheric interest of the gas phase reaction between formic acid and hydroxyl radical, there are very few theoretical investigations on its reaction mechanism. Only very recently Galano et al.[26] reported a theoretical study on the reaction mechanism, pointing out the influence of a reactant complex and the quantum mechanical tunneling effect, in the rate constant. More recently, two different theoretical works by our group focused the attention on several hydrogen bond complexes formed between formic acid and hydroxyl radical[27] and on the reaction mechanism of the acidic hydrogen abstraction by OH.[28] The latter work brings light on an unexpected reaction mechanism based on a proton coupled electron-transfer process, which can compete with a conventional hydrogen radical abstraction. In this work, we report high level theoretical calculations on the reaction mechanism, aiming to clarify the possible competition of different elementary reaction in the overall reaction. Especial emphasis has been put in the reaction modes leading to reactions 1 and 2 for which a kinetic study has been carried out.

Computational Details

Different theoretical approaches have been used in this study, employing the 6-311+G(2df,2p) basis set[29,30] in all geometry optimization. In a first step, all stationary points in the potential energy surface have been fully optimized with the hybrid density functional B3LYP method.[31] At this level of theory, we have also calculated the harmonic vibrational frequencies to verify the nature of the corresponding stationary point (minima or transition state), to provide the zero point vibrational energy (ZPE) and the thermodynamic contributions to the enthalpy and free energy. Moreover, to ensure that the transition states connect the desired reactants and products, we have performed intrinsic reaction coordinate calculations (IRC),[32−34] at this level of theory. In a second step, all stationary points were also fully re-optimized at MP2[35−37] level of theory. In addition, harmonic vibrational frequencies were also calculated for all stationary at this level of theory which also provides ZPE energies and the thermodynamic contributions to the enthalpy and entropy. In a third step, and in order to obtain more reliable geometries, we have re-optimized all stationary points at QCISD[38] level of theory. Finally, and for the shake of completeness, three transition structures of interest were optimized and characterized at CASSCF[39] level of theory. In this case, the active space (nine electrons in eight orbitals) was selected according to the fractional occupation of the natural orbitals[40] generated from an MRD-CI[41,42] wave function, which are based on the correlation of all valence electrons.

The results obtained at B3LYP and MP2 levels of theory show that, especially for the more important transition states, there are significant discrepancies in the computed imaginary frequencies, thermodynamic corrections and computed partition functions, and this fact will affect largely in doing the kinetic study. Therefore, we have carried out a further computational effort for the reactants and the four transition states that can play a key role in the reactivity between HCOOH and OH. Thus, for these stationary points we have carried out the vibrational frequency calculations at QCISD level of theory to obtain the appropriate ZPE, thermodynamic corrections and the partition functions, which are used in the kinetic study.

With the aim to get more reliable relative energies, at the geometries computed with the best theoretical treatment (QCISD/6-311+G(2df,2p)), we have performed single-point CCSD(T)[43−46] calculations using the more flexible aug-cc-pVTZ basis set.[47,48] Moreover, to obtain a better estimation of different reactant complexes found in this investigation, we have also computed, at this level of theory, the basis set superposition error (BSSE) according to the counterpoise method by Boys and Bernardi.[49]

For several stationary points of interest, we have also analyzed the bonding features by using the atoms in molecules (AIM) theory by Bader.[50] In this case, the wave function derived form the QCISD/6-311+G(2df,2p) method was employed.

Finally, the rate constants for the elementary reactions have been computed using classical transition state theory. For this purpose, we have considered the energies obtained at the CCSD(T)/aug-cc-pVTZ//QCISD/6-311+G(2df,2p) level and the partition functions computed at B3LYP, MP2, and QCISD levels of theory. The tunneling correction to the rate constants have been considered and computed by the zero-order approximation to the vibrationally adiabatic PES with zero curvature. In this case, the unsymmetrical Eckart potential energy barrier has been used to approximate the potential energy curve.[51]

(22) Benson, S. W. *Thermochemical Kinetics*; 2nd ed. ed.; Wiley-Interscience: New York, 1976.
(23) Smith, I. W. M.; Ravishankara, A. R. *J. Phys. Chem. A* **2002**, *106*, 4798.
(24) Hansen, J. C.; Francisco, J. S. *ChemPhysChem* **2002**, *3*, 833.
(25) Alvarez-Idaboy, J. R.; Mora-Diez, N.; Boyd, R. J.; Vivier-Bunge, A. *J. Am. Chem. Soc.* **2001**, *123*, 2018.
(26) Galano, A.; Alvarez-Idaboy, J. R.; Ruiz-Santoyo, M. E.; Vivier-Bunge, A. *J. Phys. Chem. A* **2002**, *106*, 9520.
(27) Torrent-Sucarrat, M.; Anglada, J. M. *ChemPhysChem* **2004**, *5*, 183.
(28) Olivella, S.; Anglada, J. M.; Sole, A.; Bofill, J. M. *Chem. Eur. J.* **2004**, in press.
(29) Frisch, M. J.; Pople, J. A.; Binkley, J. S. *J. Chem. Phys.* **1984**, *80*, 3265.
(30) Hehre, W. J.; Radom, L.; Schleyer, P. v. R.; Pople, J. A. In *Ab Initio Molecular Orbital Theory*; John Wiley: New York, 1986; p 86.
(31) Becke, A. D. *J. Chem. Phys.* **1993**, *98*, 5648.
(32) Ishida, K.; Morokuma, K.; Kormornicki, A. *J. Chem. Phys.* **1977**, *66*, 2153.
(33) Gonzalez, C.; Schlegel, H. B. *J. Chem. Phys.* **1989**, *90*, 2154.
(34) Gonzalez, C.; Schlegel, H. B. *J. Phys. Chem.* **1990**, *94*, 5523.
(35) Moeller, C.; Plesset, M. S. *Phys. Rev.* **1934**, *46*, 618.
(36) Frisch, M. J.; Head-Gordon, M.; Pople, J. A. *Chem. Phys. Lett.* **1990**, *166*, 281.
(37) Head-Gordon, M.; Head-Gordon, T. *Chem. Phys. Lett.* **1994**, *220*, 122.
(38) Pople, J. A.; Head-Gordon, M.; Raghavachari, K. *J. Chem. Phys.* **1987**, *87*, 5968.
(39) Roos, B. O. *Adv. Chem. Phys.* **1987**, *69*, 399.
(40) Anglada, J. M.; Bofill, J. M. *Chem. Phys. Lett.* **1995**, *243*, 151.
(41) Buenker, R. J.; Peyerimhoff, S. D. *Theor. Chim. Acta* **1975**, *39*, 217.
(42) Buenker, R. J.; Peyerimhoff, S. D. In *New Horizons of Quantum Chemistry*; Lowdin, P. O., Pullman, B., Eds.; D. Reidel: Dordrecht, The Netherlands, 1983; Vol. 35, p 183.
(43) Cizek, J. *Adv. Chem. Phys.* **1969**, *14*, 35.
(44) Barlett, R. J. *J. Phys. Chem.* **1989**, *93*, 1963.
(45) Pople, J. A.; Krishnan, R.; Schlegel, H. B.; Binkley, J. S. *Int. J. Quantum Chem. XIV* **1978**, 545.
(46) Raghavachari, K.; Trucks, G. W.; Pople, J. A.; Head-Gordon, M. *Chem. Phys. Lett.* **1989**, *157*, 479.
(47) Dunning, T. H. J. *J. Chem. Phys.* **1989**, *90*, 1007.
(48) Kendall, R. A.; Dunning, T. H., Jr.; Harrison, R. J. *Chem. Phys* **1992**, 6769.
(49) Boys, S. F.; Bernardi, F. *Mol. Phys.* **1970**, *19*, 553.
(50) Bader, R. F. W. *Atoms in Molecules. A Quantum Theory*; Clarendon Press: Oxford, United Kingdom, 1990.
(51) Truong, T. N.; Truhlar, D. G. *J. Chem. Phys.* **1990**, *93*, 1761.

Scheme 1. Mechanism of the Reaction between HCOOH and OH

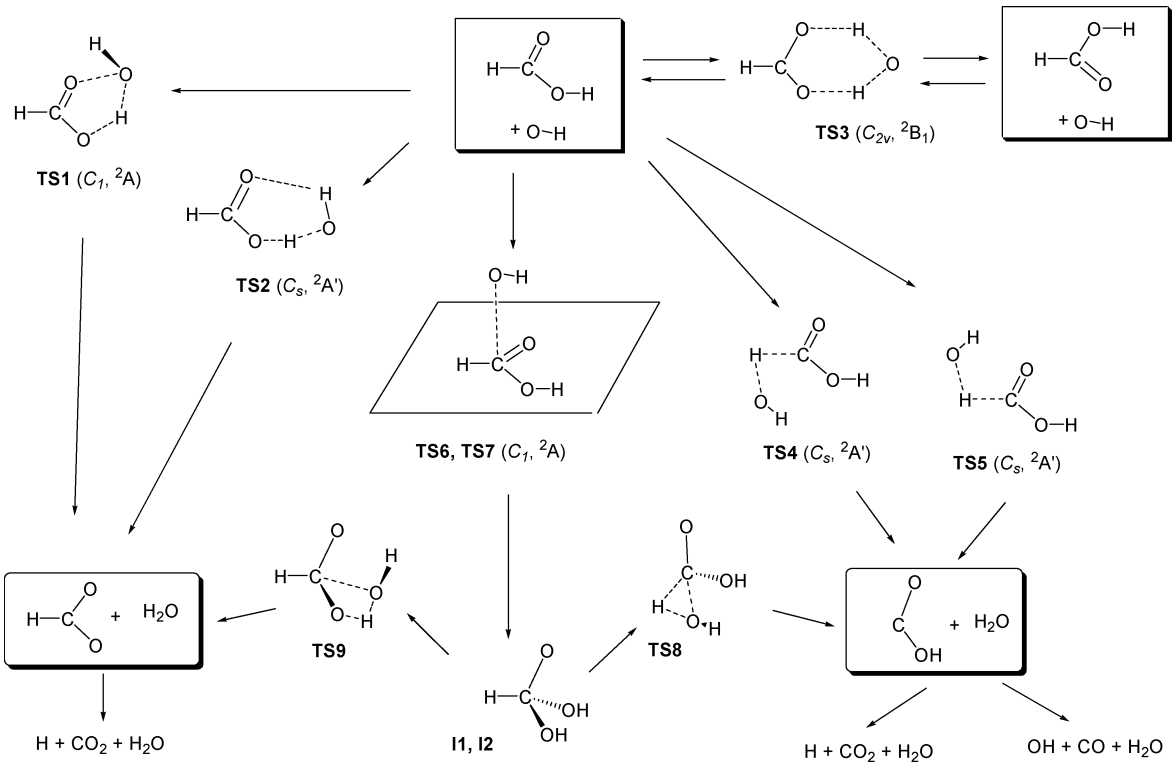

The geometry optimizations at B3LYP, MP2, and QCISD levels of theory and the CCSD(T) single point energy calculations have been performed using the Gaussian98 suit of programs.[52] The geometry optimizations at CASSCF level of theory have been done with the GAMESS program.[53] The kinetic results have been obtained with the The Rate program[54] while the topological properties of the wave function were obtained with the AIMPAC program package.[55] The Molden program[56] was also used to visualize the geometrical and electronic features of the different stationary points.

Throughout the text, all geometry discussions will refer to the QCISD/6-311+G(2df,2p) values and the energies to those computed at the CCSD(T)/aug-cc-pVTZ//QCISD/6-311+G/2df,2p) level. The geometrical parameters computed at B3LYP and MP2 levels of theory were also given in the corresponding figures for sake of comparison. The Cartesian coordinates of all stationary points, the absolute energies and the topological properties of the most relevant stationary points are also available as Supporting Information.

Results and Discussion

Most of the elementary reactions investigated in this work begin with the formation of an hydrogen bond complex, which is named by the prefix **Cr**, followed by a number; the transition states are named by the prefix **TS** followed by a number and there are also hydrogen bond complexes in the exit channel which are labeled by the prefix **Cp** followed by a number.

The different reaction paths in the potential energy surface (PES) of the HCOOH plus OH reaction are summarized in Scheme 1, which shows the complexity of the reaction mechanism. There are two reaction paths (**TS1** and **TS2**), that correspond to the acidic hydrogen abstraction producing HCOO + H_2O. A third reaction path (**TS3**) involves a simultaneous double hydrogen transfer process between HCOOH and OH, which does not produce net reaction. A fourth and fifth reaction paths (**TS4** and **TS5**) correspond to the formyl hydrogen abstraction yielding HOCO + H_2O and a sixth and seventh reaction paths (**TS6** and **TS7**) lead to the addition of hydroxyl radical to formic acid, and whose fate is the radical intermediates **I1**, **I2** ($HC(O)(OH)_2$). In addition, these radical intermediates can decompose unimolecularly, yielding HCOO + H_2O or HOCO + H_2O. The electronic features of the most important reaction paths are indicated in Scheme 2.

A schematic profile of the PES is displayed in Figure 1, which also shows the numbering of the atoms in each structure. Table 1 contains the ZPE energies, the entropies and the relative energies, enthalpies and free energies of the minima and transition states investigated as well as the values of the imaginary frequencies of the different transition states. The most relevant geometrical parameters of the stationary points considered in this work are displayed in Figures 2, 3, 4, and 5. Finally, Table 2 contains the results of the kinetic study.

Reactants and Products. Reactions 1 and 2 produce water plus formyloxyl radical (HCOO) and water plus hydroxyformyl

(52) Frisch, M. J.; Trucks, G. W.; Schlegel, H. B.; Scuseria, G. E.; Robb, M. A.; Cheeseman, J. R.; Zakrzewsk, V. G.; Montgomery, J. A. J.; Stratmann, R. E.; Buran, J. C.; Dapprich, S.; Millam, J. M.; Daniels, A. D.; Kudin, K. N.; Strain, M. C.; Farkas, O.; Tomasi, J.; Barone, V.; Cossi, M.; Cammi, R.; Mennucci, B.; Pomelli, C.; Adamo, C.; Clifford, S.; Ochterski, J.; Petersson, G. A.; Ayala, P. Y.; Cui, Q.; Morokuma, K.; Rega, N.; Salvador, P.; Dannenberg, J. J.; Malick, D. K.; Rabuck, A. D.; Raghavachari, K.; Foresman, J. B.; Cioslowski, J.; Ortiz, V.; Baboul, A. G.; Stefanov, B. B.; Liu, G. A. L.; Piskorz, P.; Komaromi, I.; Martin, R. G. L.; Fox, D. J.; Keith, T.; Al-Laham, M. A.; Peng, C. Y.; Nanayakkara, A.; Challacombe, M.; Gill, P. M. W.; Johnson, B.; Chen, W. M. W. W.; Andres, J. L.; Gonzalez, C.; Head-Gordon, M.; Replogle, E. S.; Pople, J. A.; Gaussian, Inc.: Pittsburgh, PA, 2002.
(53) Schmidt, M. W.; Baldrige, K. K.; Boatz, J. A.; Elbert, S. T.; Gordon, M. S.; Jensen, J. H.; Koseki, S.; Matsunaga, N.; Nguyen, K. A.; Su, S. J.; Windus, T. L.; Duouis, M.; Montgomery, J. A. *J. Comput. Chem.* **1993**, *14*, 1347.
(54) Duncan, W. T.; Troung, T. N.; http://therate.hec.utah.edu, downloaded September 2000.
(55) Bader, R. F. W.; http://www.chemistry.mcmaster.ca/aimpac, downloaded May 2002.
(56) Shaftenaar, G.; Noordik, J. H. *J. Comput.-Aided Mol. Desing* **2000**, *14*, 123.

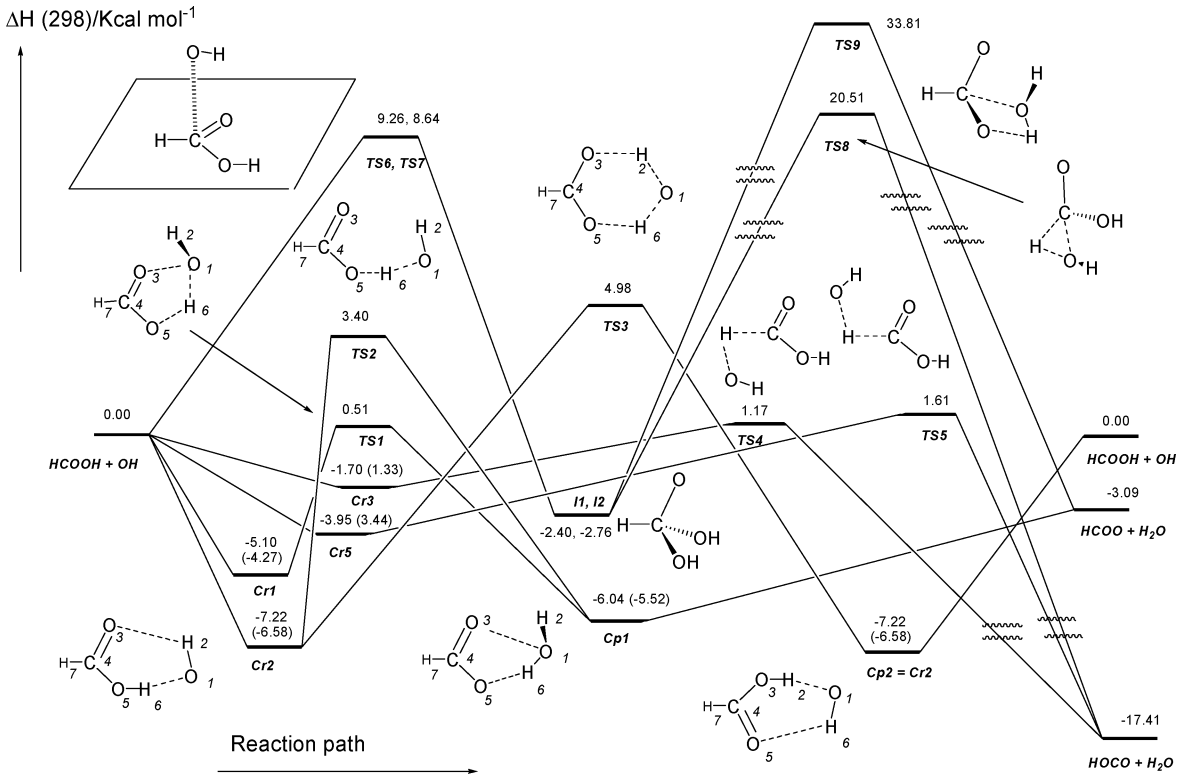

Figure 1. Schematic enthalpy diagram for the reaction between HCOOH and OH. Values in parentheses include BSSE corrections.

Scheme 2. Pictorial Representation of the Electronic Features of the Most Importat Elementary Reactions

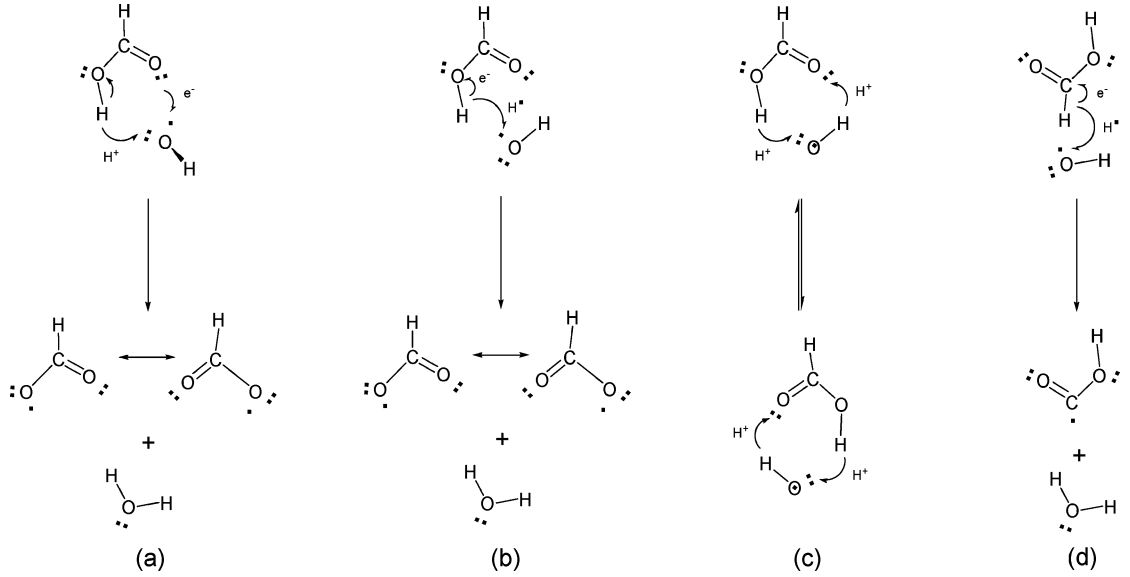

radical (HOCO), respectively. In addition, HCOO decompose yielding $H + CO_2$ whereas HOCO can produce $OH + CO$ and $H + CO_2$. These processes are of great interest for atmospheric purposes but they have been already reported in the literature.[63−69] Therefore they will not be considered in the present work.

Formyloxyl radical is a very complex system and its theoretical investigation is complicated by the symmetry-breaking problem.[59,63,70−72] In this work, we have only considered the $^2A_1$ electronic state for two reasons. First, because this is the

(57) http://webbook.nist.gov/chemistry.
(58) Kim, E. H.; Bradforth, S. E.; Arnold, D. W.; Metz, R. B.; Neumarkd, D. M. *J. Chem. Phys.* **1995**, *103*, 7801.
(59) Feller, D.; Dixon, D. A.; Francisco, J. S. *J. Phys. Chem. A* **2003**, *107*, 1604.
(60) Ruscic, B.; Schwarz, M.; Berkowitz, J. *J. Chem. Phys.* **1989**, *91*, 6780.
(61) Ruscic, B.; Litorja, M. *Chem. Phys. Lett.* **2000**, *316*, 45.
(62) Francisco, J. S. *J. Chem. Phys.* **1997**, *107*, 9039.
(63) Feller, D.; Huyser, E. S.; Borden, W. T.; Davidson, E. R. *J. Am. Chem. Soc.* **1983**, *105*, 1459.
(64) Anglada, J. M.; Crehuet, R.; Bofill, J. M. *Chem. Eur. J.* **1999**, *5*, 1809.
(65) Aoyagi, M.; Kato, S. *J. Chem. Phys.* **1988**, *88*, 6409.
(66) Forster, R.; Frost, M.; Fulle, D.; Hamann, H. F.; Hippler, H.; Schlepegrell, A.; Troe, J. *J. Chem. Phys.* **1995**, *103*, 2949.
(67) Frost, M. J.; Sharkey, P.; Smith, I. W. M. *J. Phys. Chem.* **1993**, *97*, 12254.
(68) Lester, M. I.; Pond, B. V.; Anderson, D. T.; Harding, L. B.; Wagner, A. F. *J. Chem. Phys.* **2000**, *113*, 9889.
(69) Fulle, D.; Hamann, H. F.; Hippler, H.; Troe, J. *J. Chem. Phys.* **1996**, *105*, 983.
(70) Rauk, A.; Yu, D.; Armstrong, D. A. *J. Am. Chem. Soc.* **1994**, *116*, 8222.
(71) Rauk, A.; Yu, D.; Borowski, P.; Roos, B. *Chem. Phys. Lett.* **1995**, *197*, 73.
(72) Peyerimhoff, S. D.; Skell, P. S.; May, D. D.; Buenker, R. J. *J. Am. Chem. Soc.* **1982**, *104*, 4515.

Table 1. Imaginary Frequencies (imag, in cm^{-1}), Zero Point Energies (ZPE in kcal/mol), Entropies (S in e.u.) and Reaction and Activation Energies, Enthalpies, and Free Energies (ΔE, ΔH, and ΔG in kcal/mol) for the Reaction between HCOOH and OH[a]

compound	method	imag	ZPE	S	ΔE	ΔH(298 K)	ΔG(298 K)
*syn*HCOOH + OH	B		26.4	101.9	0.0	0.0	0.0
	M		26.8	101.9	0.0	0.0	0.0
	Q		27.0	101.9	0.00	0.00	0.0
	Exp.[d]					0.00	
Cr1 (C_1, ^{2}A)	B		28.4	73.0	−6.39[b]	−5.10[b]	3.51[b]
					(−5.56)	(−4.27)	(4.34)
TS1 (C_1, ^{2}A)	B	−1325.6	26.4	68.8	1.86	0.48	10.37
	M	−2120.9	27.7	67.1	1.86	1.18	11.55
	Q	−1627.8	27.0	68.3	1.86	0.51	10.53
Cp1 (C_1, ^{2}A)	B		28.1	73.1	−7.06	−6.04	2.56
					(−6.54)	(−5.52)	(3.08)
TS2 (C_s, ^{2}A′)	M	−3121.4	25.2	69.7	6.19	3.40	13.0
Cr2=Cp2 (C_s, ^{2}A″)	B		28.3	74.0	−8.62	−7.40	0.92
					(−7.98)	(−6.76)	(1.56)
	M		28.9	73.6	−8.62	−7.22	1.20
					(−7.98)	(−6.58)	(1.84)
TS3 (C_{2v}, ^{2}B$_1$)	B	−1596.3	24.8	65.6	7.73	4.48	15.30
	M	−1664.7	25.8	65.3	7.73	4.98	15.88
Cr4 (C_s, ^{2}A′)	B		27.7	81.8	−3.15	−2.04	3.95
					(−2.66)	(−1.55)	(4.44)
	M		28.2	80.6	−3.15	−1.98	4.36
					(−2.66)	(1.49)	(4.84)
Cr3 (C_s, ^{2}A′)	B		27.2	83.5	−2.61	−1.70	3.70
					(−2.24)	(−1.33)	(4.07)
TS4 (C_s, ^{2}A′)	B	−135.4	26.5	74.4	3.67	2.91	11.12
	M	−2156.5	25.1	74.3	3.67	1.23	9.47
	Q	−1650.7	25.2	74.2	3.67	1.17	9.41
Cr5 (C_s, ^{2}A′)	B		28.0	80.1	−5.33	−4.03	2.49
					(−4.82)	(−3.52)	(3.00)
	M		28.5	80.2	−5.33	−3.95	2.51
					(−4.82)	(−3.44)	(3.02)
TS5 (C_s, ^{2}A′)	B	−133.7	26.3	75.5	4.16	3.34	11.22
	M	−2201.2	25.0	74.7	4.16	1.66	9.76
	Q	−1681.7	25.1	74.7	4.16	1.61	9.70
TS6 (C_1, ^{2}A)	B	−491.1	28.6	68.9	7.87	8.80	18.64
	M	−817.7	29.6	67.8	7.87	9.26	19.42
I1 (C_1, ^{2}A__)	B		30.1	69.5	−5.14	−2.68	6.98
	M		30.7	69.6	−5.14	−2.40	7.22
TS7 (C_1, ^{2}A)	B	−486.2	28.7	68.6	7.19	8.15	18.08
	M	−851.9	29.7	67.6	7.19	8.64	18.84
I2 (C_1, ^{2}A)	B		30.1	68.8	−5.12	−2.71	7.16
	M		30.5	68.5	−5.12	−2.76	7.18
TS8 (C_1, ^{2}A)	B	−613.0	27.4	69.3	16.45[b]	16.15[b]	25.87[b]
	M	−794.3	27.1	68.3	21.59[c]	20.51[c]	30.52[c]
TS9 (C_1, ^{2}A)	B	−1752.1	26.6	67.0	34.23[b]	32.84[b]	43.24[b]
	M	−1733.5	26.6	67.8	35.46[c]	33.81[c]	43.99[c]
HCOO ($^2A_1$) + **H_2O**	B		23.4	104.9	−2.82	−5.38	−6.26
			26.3	103.3	−2.82	−3.09	−3.51
	Exp.[d]					−7.6 ± 3.4	
cis-HOCO + H_2O	B		26.3	105.2	−17.53	−17.40	−18.39
	M		26.6	105.2	−17.53	−17.41	−18.40
	Q		26.8	105.2	−17.53	−17.38	−18.37
	Exp.[d]					−20.2 ± 1.1	
	Exp.[d]					−17.1 ± 1.3	

[a] Values in parenthesis include BSSE corrections. The Imag, ZPE, S and the contribution to the enthlaphy and free energy according to results obtained at B = B3LYP/6-311+G(2df,2p); M = MP2/ 6-311+G(2df,2p) and Q = QCISD/6-311+G(2df,2p) levels ot theory. The relative energies (ΔE) are computed at CCSD(T)/aug-cc-pVTZ//QCISD/6-311+G(2df,2p) level, while the relative enthalpies (ΔH) and free energies (ΔG) are computed adding to ΔE the corrections obtained at B, M, or Q, respectively. [b] Energies at CCSD(T)/aug-cc-pVTZ//B3LYP/6-311+G(2df,2p) level. [c] Energies at CCSD(T)/aug-cc-pVTZ//MP2/ 6-311+G(2df,2p) level. [d] The experimental reaction enthalpies are calculated taking into account the experimental $\Delta H_f°$(298 K) values of reactants and products: (−90.5 ± 0.4; 9.32; −57.80 and −31.0 ± 3 kcal/mol for HCOOH, OH, H_2O and HCOO ($^2A_1$), respectively.[57,58] For *cis*-HOCO we have added 2.9 kcal/mol (see Feller et al.[59]) to the experimental values of the trans isomer (46.5 ± 0.7 and 43.4 ± 0.9 kcal/mol, respectively[60−62]).

electronic state having the adequate symmetry that allows the further unimolecular decomposition into H + CO_2 and second, because the electronic distribution of the product complex **Cp1**, which is formed in the exit channel of **TS1** (see below), has a topology which correspond to this electronic state. Thus, this is the electronic state formed in the acidic hydrogen abstraction by hydroxyl radical. The calculations show that the $^2A_1$ electronic state is well described and characterized by the B3LYP and MP2 methods, but the QCISD approach predicts one imaginary frequency, pointing out the theoretical difficulties in describing this system.

The most relevant geometrical parameters of the reactants and products of reactions 1 and 2 are displayed in Figure 2 and compare very well with other theoretical and experimental results form the literature.[59,63,65,70−72,75] Reaction 1 has been computed to be exothermic by 3.09 kcal/mol whereas reaction 2 has been calculated to be exothermic by 17.38 kcal/mol (see Table 1 and Figure 1). These computed reaction enthalpies agree

Table 2. Calculated Values at Different Temperatures of Tunneling Parameters, κ, and Rate and Equilibrium Constants (k_{TSX} in cm^3 molecule^{-1} s^{-1}; k_{eq} in cm^3 molecule^{-1} and k_2 in s^{-1}; see eq 5) for the Processes TS1, TS2, *k*, and TS5[a]

T	298 K	300 K	320 K	340 K	360 K	380 K	400 K	420 K	440 K	460 K
					TS1					
κ	8.476	8.201	6.107	4.796	3.922	3.311	2.866	2.531	2.271	2.066
k_2	3.11×10^8	3.25×10^8	4.88×10^8	7.11×10^8	1.01×10^9	1.39×10^9	1.86×10^9	2.45×10^9	3.15×10^9	3.98×10^9
k_{eq}	1.84×10^{-21}	1.72×10^{-21}	9.20×10^{-22}	5.33×10^{-22}	3.30×10^{-22}	2.15×10^{-22}	1.48×10^{-22}	1.05×10^{-22}	7.76×10^{-22}	5.90×10^{-23}
k_{TS1}	5.72×10^{-13}	5.58×10^{-13}	4.49×10^{-13}	3.79×10^{-13}	3.32×10^{-13}	2.99×10^{-13}	2.75×10^{-13}	2.58×10^{-13}	2.45×10^{-13}	2.35×10^{-13}
					TS2					
κ	1215.800	1109.500	481.760	237.480	129.940	77.527	40.705	33.842	24.232	18.101
k_2	5.31×10^6	5.53×10^6	8.26×10^6	1.21×10^7	1.75×10^7	2.49×10^7	2.86×10^7	4.83×10^7	6.60×10^7	8.89×10^7
k_{eq}	1.84×10^{-21}	1.72×10^{-21}	9.20×10^{-22}	5.33×10^{-22}	3.30×10^{-22}	2.15×10^{-22}	1.48×10^{-22}	1.05×10^{-22}	7.76×10^{-23}	5.90×10^{-23}
k_{TS2}	9.76×10^{-15}	9.50×10^{-15}	7.60×10^{-15}	6.46×10^{-15}	5.77×10^{-15}	5.36×10^{-15}	4.22×10^{-15}	5.08×10^{-15}	5.12×10^{-15}	5.25×10^{-15}
					TS4					
κ	5.214	5.090	4.099	3.418	2.9300	2.567	2.2900	2.0720	1.898	1.755
k_2	1.09×10^9	1.11×10^9	1.35×10^9	1.63×10^9	1.93×10^9	2.26×10^9	2.63×10^9	3.02×10^9	3.44×10^9	3.88×10^9
k_{eq}	1.15×10^{-23}	1.14×10^{-23}	1.04×10^{-23}	9.71×10^{-23}	9.17×10^{-24}	8.76×10^{-24}	8.46×10^{-24}	8.24×10^{-24}	8.08×10^{-24}	7.97×10^{-24}
k_{TS4}	1.25×10^{-14}	1.26×10^{-14}	1.41×10^{-14}	1.58×10^{-14}	1.77×10^{-14}	1.98×10^{-14}	2.22×10^{-14}	2.49×10^{-14}	2.78×10^{-14}	3.09×10^{-14}
					TS5					
κ	8.890	8.593	6.343	4.947	4.024	3.382	2.917	2.569	2.300	2.089
k_2	1.19×10^8	1.24×10^8	1.85×10^8	2.70×10^8	3.84×10^8	5.33×10^8	7.22×10^8	9.59×10^8	1.25×10^9	1.60×10^9
k_{eq}	2.50×10^{-22}	2.42×10^{-22}	1.80×10^{-22}	1.40×10^{-22}	1.12×10^{-22}	9.26×10^{-23}	7.84×10^{-23}	6.77×10^{-23}	5.96×10^{-23}	5.32×10^{-23}
k_{TS5}	2.97×10^{-14}	2.99×10^{-14}	3.34×10^{-14}	3.77×10^{-14}	4.30×10^{-14}	4.93×10^{-14}	5.66×10^{-14}	6.49×10^{-14}	7.44×10^{-14}	8.50×10^{-14}
					acidic ($k_{TS1+TS2}$), formyl ($k_{TS4+TS5}$) and overall rate constant					
$k_{TS1+TS2}$	5.82×10^{-13}	5.68×10^{-13}	4.57×10^{-13}	3.85×10^{-13}	3.37×10^{-13}	3.04×10^{-13}	2.79×10^{-13}	2.63×10^{-13}	2.50×10^{-13}	2.41×10^{-13}
$k_{TS4+TS5}$	4.22×10^{-14}	4.26×10^{-14}	4.75×10^{-14}	5.35×10^{-14}	6.07×10^{-14}	6.91×10^{-14}	7.88×10^{-14}	8.98×10^{-14}	1.02×10^{-13}	1.16×10^{-13}
k_{total}	6.24×10^{-13}	6.10×10^{-13}	5.04×10^{-13}	4.39×10^{-13}	3.98×10^{-13}	3.73×10^{-13}	3.58×10^{-13}	3.52×10^{-13}	3.52×10^{-13}	3.57×10^{-13}
					branching ratio					
$\Gamma_{TS1+TS2}$	0.93	0.93	0.91	0.88	0.85	0.82	0.78	0.75	0.71	0.68
$\Gamma_{TS4+TS4}$	0.07	0.07	0.09	0.12	0.15	0.18	0.22	0.25	0.29	0.32

[a] The rate constant for the acidic hydrogen abstraction ($k_{TS1+TS2}$ in cm^3 molecule^{-1} s^{-1}), the formyl hydrogen abstraction ($k_{TS4+TS5}$ in cm^3 molecule^{-1} s^{-1}), the overall rate constant k_{total}, (in cm^3 molecule^{-1} s^{-1}), and the computed branching ratios for the acidic hydrogen abstraction ($\Gamma_{TS1+TS2}$) and the formyl hydrogen abstraction ($\Gamma_{TS4+TS5}$) are also given.The reported experimental rate constants range among 4.61 ± 0.51 and 4.34 ± 0.53: $\times 10^{-13}$ cm^3 molecule^{-1} s^{-1} between 298 and 430 K,[18] and among 4.47 ± 0.19 and 3.90 ± 0.019 $\times 10^{-13}$ cm^3 molecule^{-1} s^{-1} between 296.9 and 445.2 K.[21]

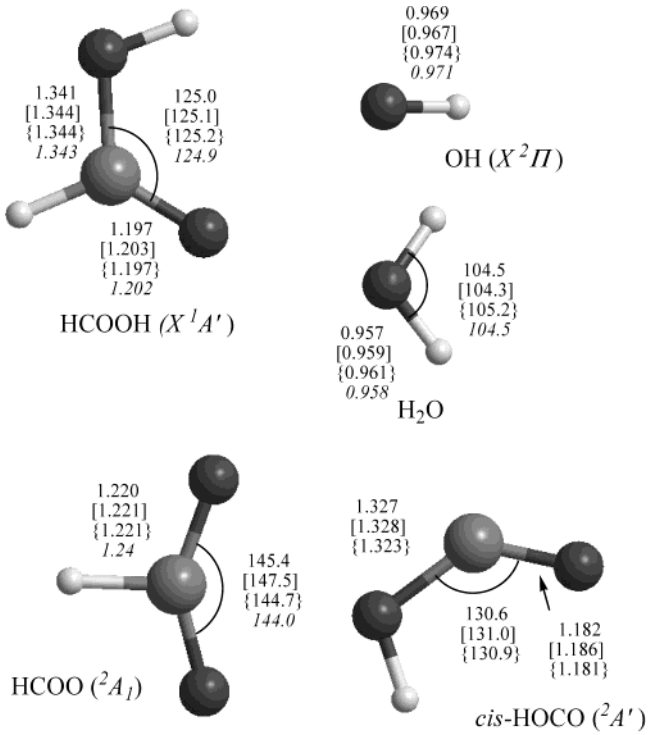

Figure 2. Selected geometrical parameters for the reactants and products, optimized at QCISD/6-311+G(2df,2p), MP2/6-311+G(2df,2p) (in brackets), and B3LYP/6-311+G(2df,2p) (in parentheses), levels of theory. Italic numbers correspond to experimental values.[58,73,74]

with the experimental heats of reaction within 1.5 kcal/mol (see Table 1), so that the expected accuracy of the activation barriers should be, at most, of this order.

Acidic Hydrogen Abstraction. This is the process indicated by reaction 1, for which we have found two different reaction paths, **TS1** and **TS2**. The computed activation enthalpies are 0.51 and 3.40 kcal/mol respectively, with respect to the reactants. These values are about 3 kcal/mol smaller than those reported recently at CCSD(T)/6-311+G(2df,2p) level of theory,[28] pointing out the importance of using a flexible basis set in order to obtain a good energetic description. Figure 1 shows that the reaction begins with the formation of the reactant complexes **Cr1** and **Cr2**, which are computed to be 5.10 and 7.22 kcal/mol, respectively, more stable than the reactants (4.27 and 6.58 kcal/mol, respectively, taking into account the BSSE correction). Additionally, there is also a product complex (**Cp1**), which is formed before the dissociation into HCOO + H_2O and that is computed to be 4.12 kcal/mol more stable than the products.

The main trends regarding the electronic features of these two transition states (**TS1** and **TS2**) and the pre-reactive hydrogen bond complex (**Cr1**) have been reported recently elsewhere.[27,28] They are also clearly reflected in the geometric features displayed in Figure 3 and in the topological parameters of the QCISD/6-311+G(2df,2p) wave function.

From a geometric point of view, **TS2** has a planar six member ring structure (C_S symmetry, $^2A'$) where the hydrogen being transferred is slightly closer the hydroxyl radical (d(O1H6) = 1.117 Å) than formic acid (d(O5H6) = 1.219 Å); see Figure 3. This transition state is also stabilized by a hydrogen bond interaction between the hydrogen of the hydroxyl radical (H2) and the oxygen of the carbonyl group (O3), (d(H2O3) = 2.071 Å), as shown by the topological analysis of the wave function (ρ = 0.0226 e.bohr^{-3} and $\nabla^2\rho$ = 0.0808 e.bohr^{-5}, see Table S1). Moreover, the two CO bond distances of the formic acid

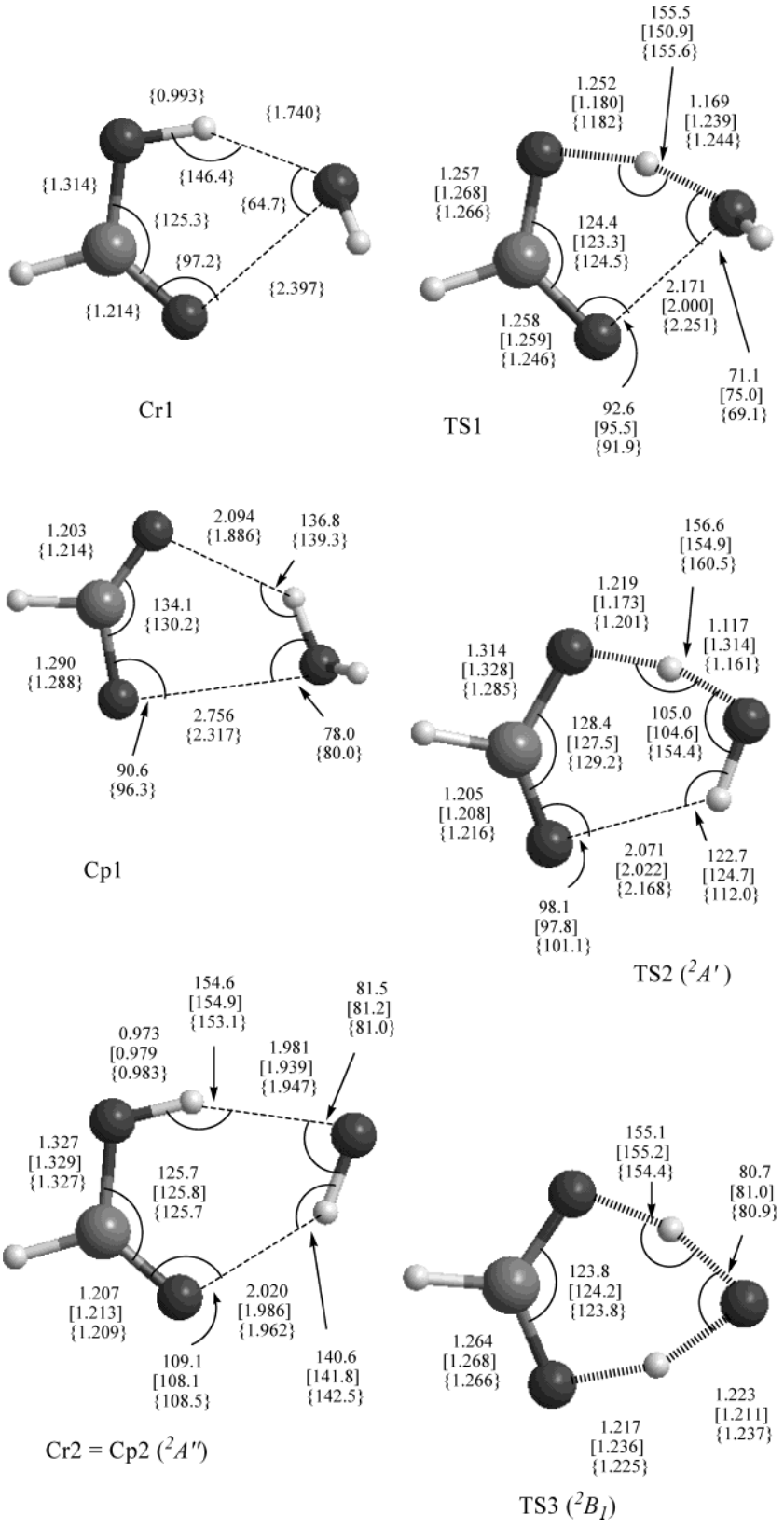

Figure 3. Selected geometrical parameters for the stationary points involving the acidic hydrogen interaction, optimized at QCISD/6-311+G(2df,2p), MP2/6-311+G(2df,2p) (in brackets), and B3LYP/6-311+G(2df,2p) (in parentheses), levels of theory.

moiety have only changed sligthly with respect to the isolated reactants (compare, for instance, from Figure 3 the bond lengths C4O5 = 1.314 Å and C4O3 = 1.205 Å in **TS2** with the corresponding distances, 1.341 and 1.197 Å respectively, in HCOOH, Figure 2). These geometrical parameters compare also with those reported recently by Galano et al.[26] As pointed out by these authors, the transition state described by **TS2** has one imaginary frequency at MP2 level of theory but two imaginary

frequencies at B3LYP levels of theory, a result that put some doubts about the true nature of this stationary point. Although it is well-known that the B3LYP method describe poorly the processes involving hydrogen transfer,[76−78] we went further by performing geometry optimization and force constants calculations at QCISD/6-311+G(2df,2p) level of theory. These calculations predict also two imaginary frequencies and seem to indicate that the doubts regarding the true nature of this stationary point cannot be ruled out. However, the fact that the QCISD frequency calculations are numerically calculated and that **TS1** lyes belolw **TS2**, could reflect a numerical problem in the **TS2** force constant matrix calculation. Therefore, we have gone further and optimized this stationary point at CASSCF/6-311+G(2df,2p) level of theory and the corresponding analytic frequency calculations predicts only one imaginary frequency. Thus, the CASSCF and MP2 results make us confident that **TS2** is a true transition state.

From an electronic point of view, the symmetry of this transition structure (C_S, $^2A'$), the analysis of the CASSCF wave function and the spin electron analysis derived from the QCISD wave function (the unpaired electron is shared between O1 (0.532) and O5 (0.428)) indicate that the reaction occurring through **TS2** involves the concerted breaking and making of the O5···H6 and H6···O1 bonds so that the reaction takes place *via the conventional hydrogen abstraction radical type mechanism*. This process is also indicated pictorially in Scheme 2b.

The process occurring through **TS1** (C_1 symmetry) is very interesting. It differs essentially from **TS2** in the orientation of the OH radical with respect to the molecular plane of formic acid, a fact that leads to a distinct electronic interaction between both reactants.[28] In **TS1**, the lone pair of the oxygen of hydroxyl radical is directed toward the acidic hydrogen of formic acid, whereas the unpaired electron of OH interacts with the oxygen of the carbonyl group forming a five-member ring structure. This ring structure is clearly identified by the topological analysis of the wave function, which shows an interesting interaction between the oxygen of the carbonyl group and the oxygen of the hydroxyl radical (the O1···O3 topological values are $\rho = 0.0482$ e.bohr^{-3} and $\nabla^2\rho = 0.1970$ e.bohr^{-5}, see Table S1). Moreover, the atomic spin population analysis indicates that the unpaired electron is shared between O1 (0.603) and O3 (0.386), in clear contrast to what happens in **TS2**. This interaction leads to a process, shown in Scheme 2a, which involves a shift of one electron of the lone pair of the oxygen of the carbonyl group to the oxygen of the hydroxyl radical, coupled with a transfer of a proton of HCOOH to OH radical,[28] that is, *this is a proton coupled electron-transfer process*. The geometrical parameters displayed in Figure 3 show that the hydrogen being transferred is also closer the hydroxyl radical (d(O1H6) = 1.169 Å) than formic acid (d(O5H6) = 1.252 Å) and the two CO bond distances of the formic acid moiety are quite the same (about 1.258 Å), indicating a larger electronic rearrangement of the π system in this process.

Here it is interesting to point out that the O1···O3 interaction described above was already present in the reactant complex **Cr1** (see the discussion in a previous work[27]), which is also stabilized by an hydrogen bond between the acidic hydrogen of formic acid and the oxygen of the hydroxyl radical. Moreover, **Cr1** presents an unexpected very large charge transfer (Δq = 101.2 me[27]) toward the hydroxyl radical, envisaging the role of this complex in the process through **TS1**. The electron transfer makes the acidic hydrogen more labile and consequently stimulates the proton transfer. In addition, the O1···O3 interaction is still present in **Cp1**, as shown by the corresponding AIM topological analysis derived from the QCISD/6-311+G(2df,2p) wave function ($\rho = 0.0116$ e.bohr^{-3} and $\nabla^2\rho = 0.0448$ e.bohr^{-5}, see Table S1).

Finally, and from a technical point of view, it should be mentioned here, that **TS1** is well described and characterized at all levels of theory considered (B3LYP, MP2, CASSCF, and QCISD).

Double Proton Transfer. Scheme 1 and Figure 1 show that the process occurring through **TS3** involves the transfer of the acidic hydrogen of formic acid to OH radical, simultaneously with the transfer of the hydrogen of the hydroxyl radical to the oxygen of the carbonyl group of formic acid. Consequently, the reactants and products are the same species so that this would be a silent reaction. However, this reaction could be experimentally observed if one of both reactants were conveniently deuterated isotopically. Thus, if OD and HCOOH were used as reactants, HCOOD and OH would be obtained as products of this reaction path whereas if OH and HCOOD were used as reactants, OD and HCOOH would be produced.

Figure 1 shows that the reaction path begins with the formation of the reactant complex (**Cr2**) which has C_s symmetry ($^2A''$), goes on through **TS3** having C_{2v} symmetry ($^2B_1$) and produces the product complex **Cp2** ($^2A''$) before the formation of HCOOH + OH. Please note that both complexes (**Cr2** and **Cp2**) in Figure 1, correspond to the same structure and consequently the reaction path is symmetric. **Cr2** has a planar six-member ring structure with two hydrogen bonds, which makes this the most stable HCOOH···OH complex (at 298 °K, $\Delta H = -7.22$ kcal/mol, or −6.58 kcal/mol considering the BSSE corrections, see Table 1, Figure 3 and also ref.[27] for a more detailed discussion on this complex). The transition state **TS3** has an activation enthalpy of 4.98 kcal/mol with respect to the reactants (see Table 1) and its geometric structure is also a symmetric six-member ring (C_{2V}, $^2B_1$, Figure 3), where both hydrogen atoms being transferred are nearly halfway between the corresponding donor and acceptor oxygen atoms. Moreover, the two C−O distances are equal (1.264 Å), pointing out the electronic redistribution of the π system along the reaction path.

From an electronic point of view, the $^2A''$ symmetry of **Cr2** and the $^2B_1$ symmetry of **TS3** imply that the unpaired electron resides, along all the reaction path, in an orbital perpendicular to the molecular plane, which is mainly localized over the oxygen of the hydroxyl radical. This is represented in Scheme 2c, which shows that the unpaired electron does no take place in the reaction and the process involves a double proton transfer.

(73) Huber, K. P.; Herzberg, G. *Molecular Spectra and Molecular Structure.*; van Nostrand: 1979; Vol. 4.
(74) Herzberg, G. *Electronic Spectra and Electronic Structure of Polyatomic Molecules*; Van Nostrand Reinhold Co.: New York, 1966.
(75) Li, Y.; Francisco, J. S. *J. Chem. Phys.* **2000**, *113*, 7963.
(76) Hamprecht, F. A.; Cohen, A. J.; Tozer, D. J.; Handy, N. C. *J. Chem. Phys.* **1998**, *109*, 6264.
(77) Tozer, D. J.; Handy, N. C. *J. Phys. Chem. A* **1998**, *102*, 3162.
(78) Sodupe, M.; Bertrán, J.; Rodriguez-Santiago, L.; Baerends, E. J. *J. Phys. Chem. A.* **1999**, *103*, 166.

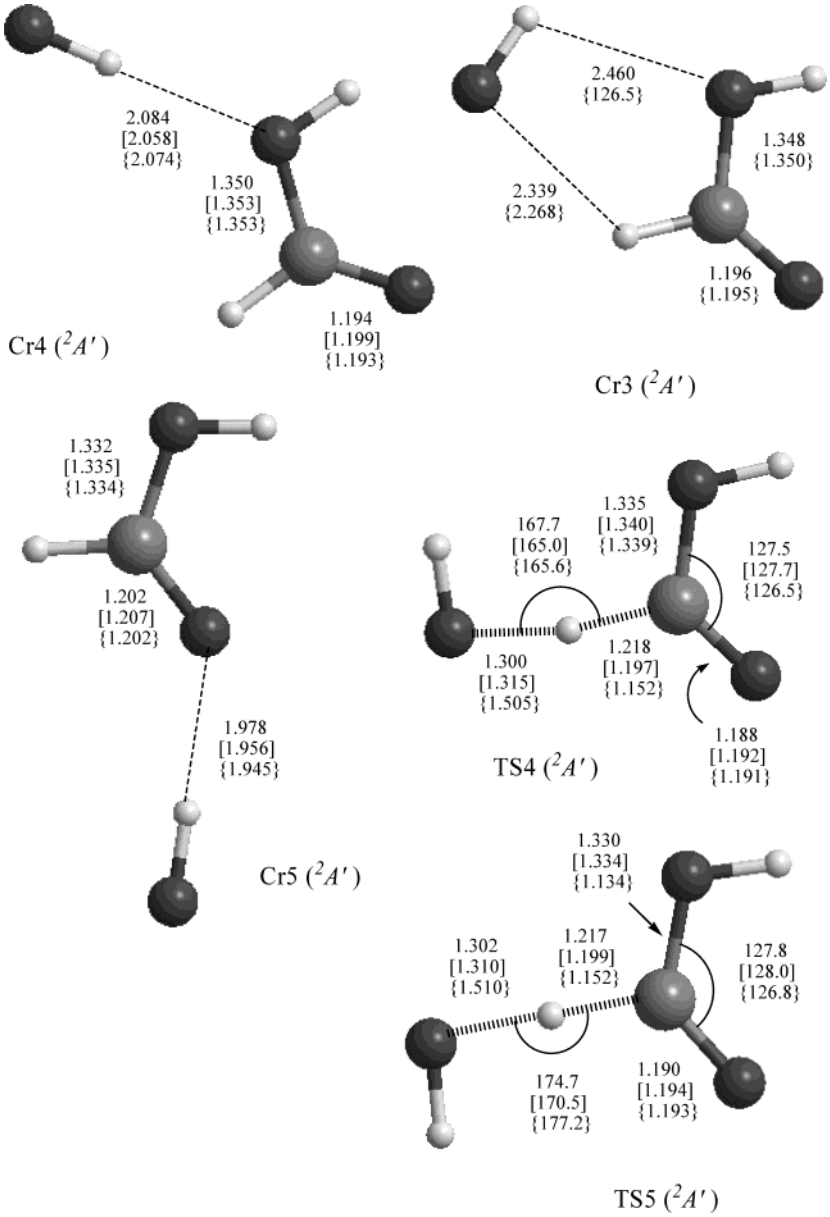

Figure 4. Selected geometrical parameters for the stationary points involving the formyl hydrogen interaction, optimized at QCISD/6-311+G(2df,2p), MP2/6-311+G(2df,2p) (in brackets), and B3LYP/6-311+G(2df,2p) (in parentheses), levels of theory.

Finally, and also from a technical point of view, it should be mentioned here, that **TS3** is well described and characterized at all levels of theory considered (B3LYP, MP2, CASSCF).

Formyl Hydrogen Abstraction. The process schematized by reaction 2, corresponding to the formyl hydrogen abstraction by OH, has two reaction paths as shown in Scheme 1 and Figure 1. The two transition states (**TS4** and **TS5**) have a planar structure (symmetry C_S, ^{2}A′), and differentiate from each other by the relative orientation of the hydroxyl radical with respect to formic acid, toward the hydroxyl or the carbonyl group of HCOOH, respectively. Both processes involve a *conventional hydrogen abstraction radical type mechanism* (see Scheme 2d), that is, the concerted braking and making of the C−H and O−H bonds. The geometrical parameters displayed in Figure 4 show that in both cases (**TS4** and **TS5**), the hydrogen atom being transferred is closer the carbon of formic acid than the oxygen of hydroxyl radical (d(CH) about 1.22 Å and d(HO) about 1.30 Å), whereas the CO bond distances of the formic acid moiety have only changed sligthly with respect to the isolated reactants. Moreover, their geometrical structures suggest the possibility that both transition structures may be stabilized by a hydrogen bond interaction as described in **TS2**. However, the AIM analyses of the corresponding wave function indicate that such H-bond interaction does not occur.

For **TS4**, we have calculated an activation enthalpy of 1.17 kcal/mol, with respect to the reactants, and the reaction begins with the reactant complex **Cr3**, which is 1.70 kcal/mol below the reactants (1.33 kcal/mol considering the BSSE correction; ΔH values, see Table 1). Close to **Cr3**, there is also another complex (**Cr4**) with the same relative orientation of the HCOOH and OH moieties and which is slightly more stable (1.98 or 1.49 kcal/mol considering the BSSE correction, see Table 1). The structure of both complexes is displayed in Figure 4 and a more detailed discussion is reported elsewhere.[27]

In the case of **TS5**, the computed activation enthalpy is slightly higher (1.61 kcal/mol) and the reactant complex (**Cr5**)

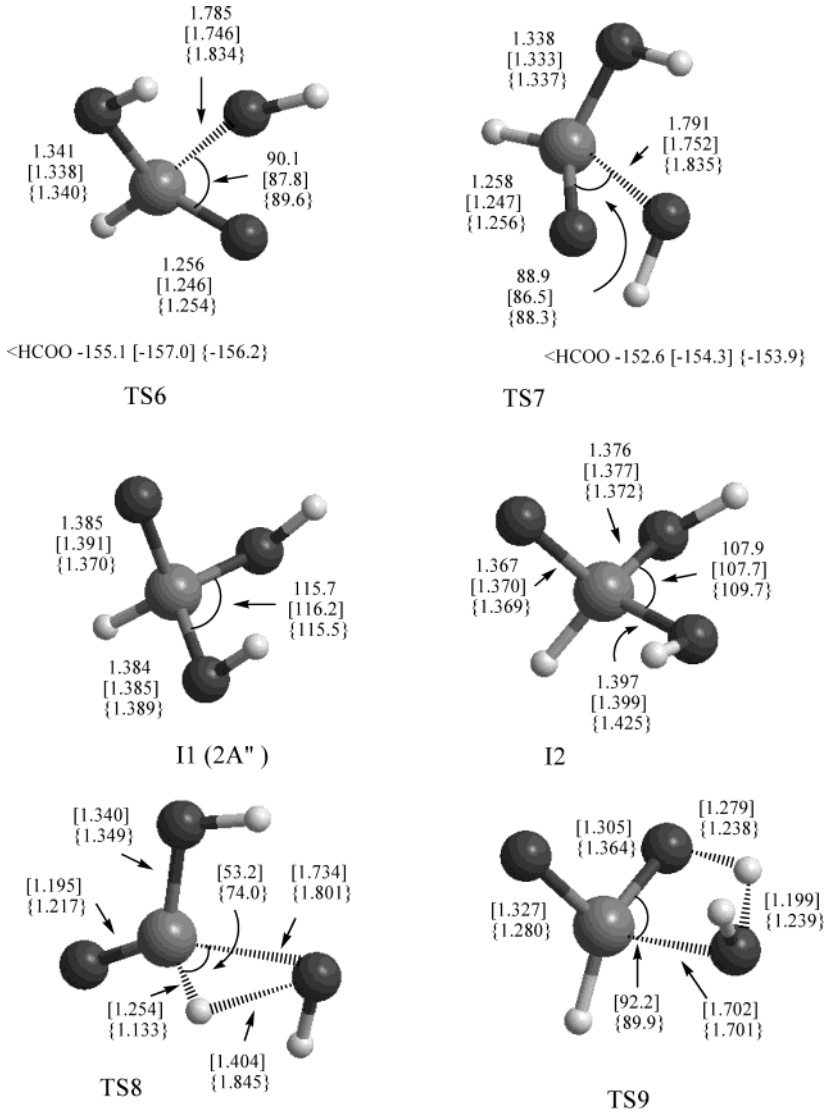

Figure 5. Selected geometrical parameters for the stationary points involving the addition of OH to formic acid, optimized at QCISD/6-311+G(2df,2p), MP2/6-311+G(2df,2p) (in brackets), and B3LYP/6-311+G(2df,2p) (in parentheses), levels of theory.

is computed to be 3.95 kcal/mol more stable than the reactants (3.44 kcal/mol considering the BSSE correction). The main features regarding these pre-reactive H-bond complexes have been recently described in the literature[27] and for **Cr5** and **TS5**, our results compare with those reported recently by Galano et al.[26]

At this point, it is also important to note the reader that the activation enthalpies of **TS4** and **TS5** (1.17 and 1.61 kcal/mol, respectively) are smaller than those of **TS2** (3.40 kcal/mol), the three processes having a conventional hydrogen abstraction radical type mechanism. These results agree with what was expected according to the strength of the C−H and O−H bonds in formic acid (see above), although the small difference in the activation enthalpies (**TS4** and **TS5** versus **TS2**; about 2 kcal/mol) can be attributed to the hydrogen bond interaction in **TS2**, which produces a stabilization effect. Moreover, the results reported in this work allow clarifying the not understood experimental fact that the OH radical interact mainly with the carboxylic hydrogen. The existence of a different process occurring through **TS1**, with smaller activation enthalpy (0.51 kcal/mol) and that does not involve a conventional hydrogen abstraction radical type mechanism (see above) explain the unexpected experimental observation regarding the higher reactivity of formic acid with OH radical.

OH Addition to Formic Acid. Wine et al.[18] postulated the possibility that the reaction between HCOOH and OH could occur, in a first step, by addition of hydroxyl radical to formic acid and this process has been also considered in the present work (see Scheme 1 and Figure 1). We have found two reaction paths for the addition reaction, whose corresponding transition states are labeled by **TS6** and **TS7**, and differentiate form each other in the relative orientation of the OH radical with respect formic acid. Their fate are the intermidiates **I1** and **I2**, corresponding to two different conformers of $HCO(OH)_2$. Both reaction paths involve the radical addition to the carbon atom of formic acid by interaction with the π bond of the carbonyl group, so that the unpaired electron in the resulting **I1** and **I2** intermediates is mainly located on the terminal oxygen. This is clearly reflected in the geometrical parameters of the corresponding stationary points. Regarding the transition structures **TS6** and **TS7**, Figure 5 shows a significant pirimidalization of the formic acid moiety (about 25°), which is produced by bond

formation between the carbon atom and the oxygen of the hydroxyl radical (d(C−O) = 1.785 and 1.791 Å, for **TS6** and **TS7**, respectively). At the same time, the CO bond of the carbonyl group is enlarged by about 0.06 Å with respect to HCOOH, pointing out the π bond is being broken. From an energetic point of view, the intermediates **I1** and **I2** are computed to be exothermic by about 2.7 kcal/mol, and the calculated activation enthalpies are 9.26 and 8.64 kcal/mol for **TS6** and **TS7** respectivelly, see Table 1. These energy barriers are significatnly higher than the direct hydrogen abstraction processes described above making this process unlike.

For the shake of completeness, we have also considered the unimolecular decomposition of the $HCO(OH)_2$ (**I1** and **I2**) intermediate. In this case the geometry optimizations have been carried out only at B3LYP/6-311+G(2df,2p) and MP2/6-311+G(2df,2p) level. We have found two different elementary reactions, namely via **TS8** yielding HOCO + H_2O and via **TS9** producing HCOO + H_2O. The corresponding transition structures are displayed in Figure 5 and the computed activation enthalpies are even higher (22.91 and 36.57 kcal/mol respectivelly, referred to the $HCO(OH)_2$ intermediate; see Table 1 and Figure 1).

Kinetics. The results discussed in the previous secction suggest the posibility that different elementary reactions could contribute to the overall HCOOH plus OH reaction. In particular, reactions occurring through **TS1**−**TS5**, have the lowest activation enthalpies and may have some contribution to the rate constant. Therefore, we have employed the conventional transition state theory in order to estimate the possible competition of each elementary reaction and to compute the overall rate constant. The rate constants have been calculated in the range of temperatures between 298 and 460 K.

We have shown in the previous sections that, in each case, a barrier-less reactant complex is formed before the hydrogen abstraction by hydroxyl radical. Thus, every process (I) is a complex reaction as described by eq 4, where the complex is in equilibrium with the reactants.

$$\mathrm{HCOOH} + \mathrm{OH} \underset{k_{-1}}{\overset{k_1}{\rightleftharpoons}} \text{reactant complex} \xrightarrow{k_2} \text{product} + \mathrm{H_2O} \tag{4}$$

The free energy results displayed in Table 1 suggest that the reactant complexes are, in part, shifted to the reactants, so that the rate constant for each process is given by eq 5.

$$k_I = \frac{k_1}{k_{-1}} k_2 = K_{eq} k_2 \tag{5}$$

The equilibrium constant K_{eq} in the first step and the rate constant k_2 of the second step of eq 4 are given by eqs 6 and 7 respectively

$$K_{eq} = \frac{Q_{complex}}{Q_{HCOOH} Q_{OH}} e^{(-(E_C - E_R)/RT)} \tag{6}$$

$$k_2 = \kappa \frac{k_b T}{h} \frac{Q_{TS}}{Q_{complex}} e^{(-(E_{TC} - E_c)/RT)} \tag{7}$$

Where the various Q denote the partition functions of the reactants HCOOH and OH, the hydrogen bond complex and the transition state; E_R, E_C, and E_{TS} are the total energies of the reactants, hydrogen bond complex and transition state, respectively, k_b and h are the Boltzmann and Planck constants, respectively, and κ is the tunneling parameter.

In doing the kinetic study for reactions **TS1** through **TS5**, we have considered for the calculations of k_2 (eq 7) the reactant complex that is formed previous each transition state (that is, **Cr1** for **TS1**, **Cr2** for **TS2** and **TS3**, **Cr3** for **TS4**, and **Cr5** for **TS5**), whereas for the equilibrium between the complex and the reactants (eq 6), we have taking into account the more stable complex having the correct orientation (that is, **Cr3** for **TS1**, **TS2** and **TS3**; **Cr4** for **TS4**, and **Cr5** for **TS5**).

For the equilibrium constant calculations the BSSE correction for the relative stabiblity between reactants and complexes were considered and the MP2 partition functions were employed. An important point in computing the k_2 rate constant is to choose the theoretical level at which the partition functions have to be computed, specially at the transition state. This is because the curvature of the PES at this point has also a direct influence on the computed tunneling parameter. Preliminar calculations employing partition functions computed at B3LYP and MP2 levels of theory result in values of the computed rate constants that differ in a factor of about 100, and showed that **TS3** does not contribute to the overall rate constant. These large discrepancies in the computed rate constants were to be expected taking into account the different description of the transition states by the two mentioned theoretical approaches, specially for **TS4** and **TS5**. Thus, for these transition state structures, the values displayed in Table 1 show very large differences in the computed value of the imaginary frequency corresponding to the transition vector. Moreover, the discrepancies in the enthalpic and entropic corrections are also significative. Therefore we have done an extra computational effort and for the transition states **TS1**, **TS2**, **TS4**, and **TS5**, we have carried out frequency calculations at the QCISD/6-311+G(2df,2p) theoretical level. For **TS1**, **TS4**, and **TS5** the QCISD/6-311+G(2df,2p) partition functions were used. For **TS2**, the QCISD frequency calculations result in two inaginary frequencies (see above) and therefore the MP2 partition functions were employed. Here, for the reactant complexes, we have used the B3LYP partition functions because this information can be computed for all reactant complexes (see above).

The overall rate constant ($k_{total} = k_{TS1} + k_{TS2} + k_{TS4} + k_{TS5}$) computed at 298 K is 6.24×10^{-13} cm^3 molecules^{-1} s^{-1}, which compares quite well with the range $3.2 \pm 1 - 4.9 \pm 1.2 \times 10^{-13}$ cm^3 molecules^{-1} s^{-1}, reported experimentally. This value compares also with the computed rate constant reported recently by Galano et al., although these authors predict a mechanism based on **TS2**. The discrepancies between our results and those by, Galano et al.[26] are due to the fact that they computed the activation barrier, using a smaller basis set, results in an activation barrier which is about 2 kcal/mol larger, and produces a too large tunneling coefficient and therefore an overestimation of the computed rate constant for this elementary mechanism.

The calculations reported in this work predict also a small temperature dependence of the rate constant (a factor of 1.75 between 280 and 460 K), whereas the experimental rate constant is nearly temperature independent (see Table 2). This discrepancy may be addressed to the fact that partition functions computed at different theoretical levels have been used for

reactant complexes and transition states and perhaps more important, for using classical transition state theory in the kinetic study. The use of variational transition state theory would provide better results, although this is outside the reasonable computer facilities if the partition functions have to be computed at QCISD/6-311+G(2df,2p) level of theory.

With regard to the particular processes contributing to the rate constant, the results displayed in Table 2 shows that the dominant process is the acidic hydrogen abstraction ($k_{TS1} + k_{TS2}$), but the importance of the formyl hydrogen abstraction ($k_{TS4} + k_{TS5}$) increases with temperature as observed experimentally. Thus, as displayed in Table 2, we have computed a branching ratio for the acidic hydrogen abstraction [$\Gamma_{acidic} = (k_{TS1} + k_{TS2})/k_{total}$], of 93.2% at 298 K, which decreases to 67.5% at 460 K. A further interesting point refers to the acidic hydrogen abstraction (reaction 1). The values of Table 2 show clearly that this reaction occur almost exclusively through **TS1**, whereas the process through **TS2** contribute to reaction 1 in less than 2% over all temperature range considered.

Summary and Conclusions

The extensive theoretical study carried out on the reaction between formic acid and hydroxyl radical, which is of interest in atmospheric chemistry, lead to the following conclusions:

The gas-phase reaction between HCOOH and OH has a very complex reaction mechanism. There are five elementary processes involving a direct interaction between hydroxyl radical and one of the two hydrogen atoms of formic acid, and these processes have different and very interesting features form an elelctronic point of view. Each of these elementary process is itself a complex reaction since begins with a barrierless first step leading to the formation of a reactant complex, and a second step where one hydrogen of HCOOH is extracted by OH radical.

There are two elementary reaction for the abstraction of the acidic hydrogen (reaction 1). **TS1** has the lowest activation enthalpy (0.51 kcal/mol) and electronically the reaction involves a *proton coupled electron-transfer process* (PCET). The second elementary reaction **TS2**, has an activation enthalpy of 3.40 kcal/mol and involves a *conventional hydrogen radical abstraction* process.

There is a process (**TS3**), with a computed activation enthalpy of 4.98 kcal/mol, which involves a simultaneous double proton transfer between HCOOH and OH, and does not produce net reaction.

There are two reaction paths (**TS4** and **TS5**) for the formyl hydrogen abstraction (reaction 2) with computed activation enthalpies of 1.17 and 1.61 kcal/mol, respectively. Both elementary reactions involve a conventional hydrogen radical abstraction mechanism by OH radical.

There are also two reaction paths (**TS6** and **TS7**) involving the OH addition to formic acid, but these processes have higher activation enthalpies and therefore are unlike.

Our results shows clearly that the formyl hydrogen atom abstraction (**TS4** and **TS5**) have smaller activation enthalpies than the acidic hydrogen atom abstraction (**TS2**), as expected according to the their respective experimental BDE values.

The kinetic analisys carried out in this work reproduce the experimental trends relative to the fact that the dominant interaction of the OH radical is with the acidic hydrogen (reaction 1) and that the abstraction of the formyl hydrogen (reaction 2) increases its contribution at higher temperatures. The predominant reaction 1 is due to a proton coupled electron-transfer process, having a smaller activation enthalpy than the hydrogen atom abstraction ocurring in reaction 2. However our calculations predict a small temperature dependence in contranst to the experimantal results.

Finally, the computed rate constant at 298 K is 6.24×10^{-13} cm^3 $molecules^{-1}$ s^{-1}, and compares quite well with the experimental values.

Acknowledgment. The financial support for this work was provided by the Dirección General de Investigación Científica y Técnica (DGYCIT, Grant No. BQU2002-0485-C02-01) and by the Generalitat de Catalunya (Grant No. 2001SGR00048). The calculations described in this work were performed at the Centre de Supercomputació de Catalunya (CESCA) and the Centro de Supercomputación de Galicia (CESGA), whose services are gratefully acknowledged. I am indebted to prof. S. Olivella and Prof. J. M. Bofill for helpful discussions.

Supporting Information Available: Absolute energy values, Topological parameters of selected stationary points and optimized geometries. This material is available free of charge via the Internet at http://pubs.acs.org.

JA0481169